ANALYSIS OF REACTIVE FLOW IN SOLID FUEL RAMJET COMBUSTORS

Hélio de Miranda Cordeiro
Instituto de Pesquisa e Desenvolvimento – GQ/IPD, 23010-470 – Guaratiba, RJ, Brazil, hcordeir@ipd.eb.mil.br

Angela Ourivio Nieckele
Department of Mechanical Engineering, Pontifical Catholic University of Rio de Janeiro, 22453-900 – Rio de Janeiro, RJ, Brazil, nieckele@mec.puc-rio.br

Abstract. *A numerical analysis of reactive and turbulent flow field in a solid fuel ramjet combustor is presented. The mathematical model is based on the numerical solution of the conservation equations of mass, momentum, energy and transport equations for scalar quantities. The κ–ε turbulence model for high Reynolds is employed and the combustion is modeled with the mixture fraction/prescribed probability density function formalism. Close to the walls a law-of-the-wall is specified, with the boundary layer divided into two regions, a viscous sublayer and a fully turbulent region. Heat and mass transfer at the walls are calculated using a modified law-of-the-wall based on a blowing parameter. The solid fuel ramjet has three regions, the air intake, the combustor and the exhaust nozzle. The proposed model was applied to different ramjet configurations, and the regression rate along the fuel surface was determined. The results obtained were compared with available numerical and experimental data presenting good agreement.*

Key-words: *Combustion, solid fuel, ramjet, computational analysis*

1. INTRODUCTION

The solid-fuel ramjet (SFRJ) is currently being considered as the propulsion device for a number of tactical applications, such as missiles and gun-launched projectiles, since the ramjet with subsonic combustion is considered the simplest and hence the most reliable and the least expensive propulsion device for supersonic flight. Figure (1) shows the typical configuration of solid fuel ramjet. The SFRJ may utilize a sudden dump inlet for flame stabilization and some means of mixing downstream of the fuel grain in order to burn all of the available fuel that is in the gas phase.

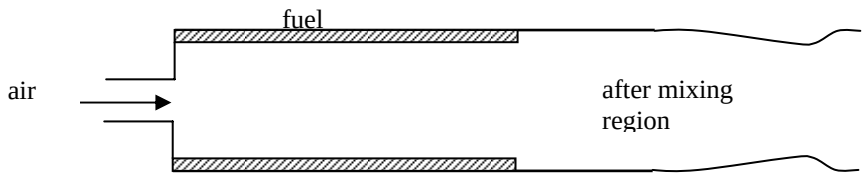

Figure 1. Typical configuration of a solid fuel ramjet.

Combustion aspects of solid fuel ramjet (SFRJ) are reviewed by Krishnan and George (1998). The use of solid fuels in ramjets was investigated experimentally by Netzer (1977), Gobbo-Ferreira et al. (1999), Pelosi-Pinhas and Gany (2003), and Ciezki (2003), among others. They studied the influence of several parameters, as chamber pressure, inlet air temperature and the gas mass flow rate on the fuel regression rate. Stevenson and Netzer (1981) established theoretical models for the combustion process in such systems. Elands et al. (1990) modeled the flow and combustion

processes in a SFRJ and validated the model against experimental results. Cordeiro and Nieckele (2003) investigated the prediction of solid fuel pyrolisis with different models and found that the model proposed was suitable for the prediction of mass transfer and flow field in a solid fuel ramjet combustor.

The objective of this paper is to investigate different ramjet configurations. The simulation yields information about velocity, temperature and scalar variables flow field. The solid fuel regression rate at the solid fuel wall is also estimated.

2. THE MATHEMATICAL MODEL

The flow was assumed to be subsonic, two-dimensional and steady, that is, transient effects were neglected. The viscous work was neglected since low Mach number flow approach was used. Soret and Dufour effects were neglected such as radiant heat transfer.

The mathematical model is based on the solution of the Favre-averaged conservation equations for mass and momentum, energy and transport equations for scalar quantities.

$$\frac{\partial}{\partial x_i}(\bar{\rho}\tilde{u}_i) = 0 \quad ; \quad \frac{\partial}{\partial x_j}(\bar{\rho}\tilde{u}_j\tilde{u}_i) = \frac{\partial}{\partial x_j}\left(\mu_t \frac{\partial \tilde{u}_i}{\partial x_j}\right) + \frac{\partial}{\partial x_j}\left(\mu_t \frac{\partial \tilde{u}_j}{\partial x_i}\right) - \frac{\partial \bar{P}}{\partial x_i} \tag{1}$$

$$\frac{\partial}{\partial x_j}(\bar{\rho}\tilde{u}_j\tilde{H}) = \frac{\partial}{\partial x_j}\left[\frac{\mu_t}{\sigma_t}\left(\frac{\partial \tilde{H}}{\partial x_j}\right)\right] \quad ; \quad \frac{\partial}{\partial x_i}\left(\bar{\rho}\ \tilde{u}_i\ \tilde{f}\right) = \frac{\partial}{\partial x_i}\left(\frac{\mu_t}{\sigma_f}\frac{\partial \tilde{f}}{\partial x_j}\right) \tag{2}$$

where $\bar{\rho}$ is the mean gas density, $\tilde{u}_i$ and $\tilde{u}_j$ are mean mass average velocity components, $\bar{P} = \bar{p} + (2/3)[(\mu_t\ \partial \tilde{u}_k / \partial x_k) + (\bar{\rho}\kappa)]$ is a modified pressure, where $\bar{p}$ is the combustor mean pressure, and μ_t is the turbulent viscosity. $\tilde{H}$ is the mean stagnation enthalpy given by $\tilde{H} = \tilde{h} + \tilde{u}_i\tilde{u}_i/2 + \kappa$, $\tilde{h}$ is the mean specific enthalpy and $\tilde{f}$ is the average mixture fraction. σ_t and σ_f are empirical constants. μ_t can be obtained by $\mu_t = C_\mu\ \bar{\rho}\ \kappa^2/\varepsilon$ (Launder and Spalding, 1976), where C_μ is an empirical constant. It requires that two additional transport equations (for turbulence kinetic energy, κ, and its dissipation rate, ε) be evaluated.

$$\frac{\partial}{\partial x_j}(\bar{\rho}\tilde{u}_j\kappa) = \frac{\partial}{\partial x_j}\left[\frac{\mu_t}{\sigma_k}\frac{\partial \kappa}{\partial x_j}\right] + P_\kappa - \bar{\rho}\varepsilon \quad , \quad \frac{\partial}{\partial x_j}(\bar{\rho}\ \tilde{u}_j\varepsilon) = \frac{\partial}{\partial x_j}\left[\frac{\mu_t}{\sigma_\varepsilon}\frac{\partial \varepsilon}{\partial x_j}\right] + C_1\frac{\varepsilon}{\kappa}P_\kappa - C_2\bar{\rho}\frac{\varepsilon^2}{\kappa} \tag{3}$$

where P_κ is the turbulent kinetic energy production term defined by

$$P_k = -\overline{\rho u_i'' u_j''}\frac{\partial \tilde{u}_i}{\partial x_j} = \mu_t\left(\frac{\partial \tilde{u}_i}{\partial x_j} + \frac{\partial \tilde{u}_j}{\partial x_i}\right)\frac{\partial \tilde{u}_i}{\partial x_j} - \frac{2}{3}\left[\mu_t\left(\frac{\partial \tilde{u}_k}{\partial x_k}\right) + \bar{\rho}\ \kappa\right]\frac{\partial \tilde{u}_i}{\partial x_j}\delta_{ij} \tag{4}$$

The empirical constants of model are C_1=1.43, C_2=1.92, C_μ=0.09, σ_t =0.7; σ_κ=1.0 and σ_ε=1.3 (Launder and Spalding, 1973).

Combustion is modeled using the conserved scalar/presumed probability density function (p.d.f.) formalism. It is assumed that combustion is described by a single one-step irreversible reaction between the fuel and the oxidizer yielding combustion products. Therefore the combustion process is mixing limited. This assumption provides relationships between the instantaneous values of chemical species concentrations and the conserved scalar, taken as the mixture fraction.

The mean values of the species mass fraction and gas mixture temperature may be found from

$$\tilde{\phi} = \int_0^1 \phi(f)\,p(f)\,df \tag{5}$$

where $\tilde{\phi}$ is the variable mean value, $\phi(f)$ is the variable instantaneous value and f is the mixture fraction. When the variable is mass fraction, $\phi(f)$ is obtained from state relationships. The instantaneous gas mixture temperature is function of mixture enthalpy and mixture fraction, $\phi(h, f)$. $p(f)$ is the probability density function based on the normalized Beta function (Wolfram, S. 2002), depending on the mean mixture mass fraction $\tilde{f}$ and its variance g_f, which must be obtained from its conservation equation

$$p(f) = \frac{f^{a-1}(1-f)^{b-1}}{\int_0^1 f^{a-1}(1-f)^{b-1} df} \quad ; \quad a = \tilde{f}\left[\frac{\tilde{f}(1-\tilde{f})}{g_f} - 1\right] \quad ; \quad b = \frac{a(1-\tilde{f})}{\tilde{f}} \tag{6}$$

$$\frac{\partial}{\partial x_j}(\bar{\rho}\tilde{u}_j g_f) = \frac{\partial}{\partial x_j}\left(\frac{\mu_t}{\sigma_t}\frac{\partial g_f}{\partial x_j}\right) - 2\frac{\mu_t}{\sigma_t}\left(\frac{\partial \tilde{f}}{\partial x_j}\right)^2 - 2\bar{\rho}\frac{\varepsilon}{\kappa}g_f \tag{7}$$

The mean gas density was calculated using the equation of state

$$\bar{\rho} = \frac{\bar{p}/(\Re \tilde{T})}{\sum_j \tilde{m}_j / M_j} \tag{8}$$

where $\Re$ is the universal gas constant, M_j is the molecular mass of j specie and $\tilde{T}$ is the mean gas mixture temperature.

3. GEOMETRY AND BOUNDARY CONDITIONS

Figure (2) shows schematically the geometric parameters of combustor. The partial differential equations can be solved if the required boundary conditions are specified. At the inlet was assumed uniform distribution for all variables. At the outlet and the centerline of the combustor, a no-gradient condition was used for all equations except the *r*-momentum equation for which a zero velocity is specified. All solid boundaries present no slip condition (both velocity components equal to zero), in addition, were considered adiabatic and impermeable except the solid fuel surface where mass injection (also called blowing) occurs due to fuel regression.

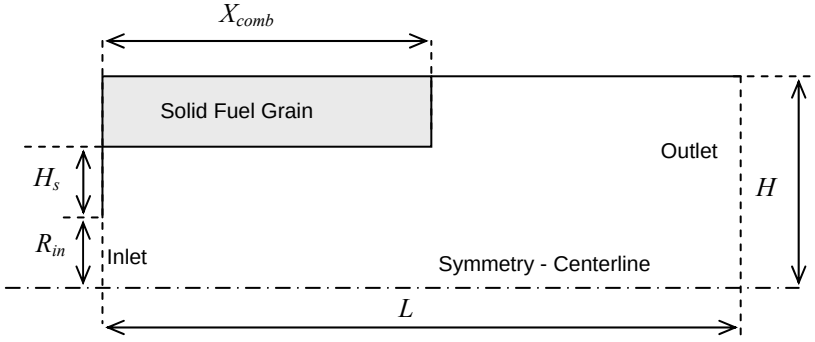

Figure 2. Geometric parameters of computational domain.

3.1. Adiabatic and Impermeable Walls

The diffusive flux through the walls for $\tilde{H}$, $\tilde{f}$ and g_f variables were considered equal to zero. Near solid walls, viscous effects become important due to no slip condition. Thus, κ–ε turbulence model is not valid close to the walls, where Reynolds number is low.

For simplicity, a two-region boundary layer was used. The border between the laminar sub layer and the fully turbulent layer was taken at y^+=11.5. This dimensionless variable was defined by

$$y^+ = \frac{\overline{\rho}\ y_P\ (\tau_w / \overline{\rho})^{1/2}}{\mu} \tag{9}$$

where y_p is the near-wall node distance from the wall, τ_w is the wall shear stress and $\overline{\rho}$ is evaluated at y_p. The fully turbulent region is taken at $y^+ \geq 11.5$.

Defining a dimensionless axial velocity by $u^+ = \tilde{u}_P / \sqrt{\tau_w / \overline{\rho}}$, for stationary and two-dimensional boundary layer without gradient pressure and blowing or suction, the following equations can be used near the wall region:

If $y^+ \geq 11.5$ then $$u^+ = \frac{1}{k} \ln (E\ y^+) \tag{10}$$

If $y^+ < 11.5$ then $$u^+ = y^+ \tag{11}$$

where k =0.4 is the von Kárman constant and $E \approx 9$.

In the fully turbulent region, it was assumed equilibrium between the production and the destruction of turbulent kinetic energy. As a consequence, turbulent kinetic energy is proportional to the wall shear stress, which is approximately constant in the near wall region. Therefore, the following equations were applied to calculate the turbulent kinetic energy and its dissipation rate at the near wall region, where the subscript P means first internal node point.

$$\frac{\partial \kappa}{\partial y} = 0 \quad ; \quad \varepsilon_P = \frac{C_\mu^{3/4} \kappa_P^{3/2}}{k\ y_P} \tag{12}$$

3.2 Solid Fuel Surface

The pyrolizing fuel causes a mass flux of fuel from the wall to the main flow, where the fuel is burnt. The blowing velocity can be evaluated from

$$v_w = \frac{\dot{q}_w}{\overline{\rho}_{fu-g} H_{v,eff}} \tag{13}$$

where $\dot{q}_w$ is heat flux to the wall, $\overline{\rho}_{fu-g}$ is the density of gaseous fuel and $H_{v,eff}$ is the effective heat of gasification, i.e., the amount of heat required to pyrolize 1 Kg of fuel. Because of the blowing velocity, the wall functions early presented cannot be used, and a modified wall function is used to account for the blowing effects.

The assumptions employed for reacting flows result in the following general boundary condition for all "conserved" variables (ϕ_c) on a surface which has mass transfer (Kays, 1966)

$$\dot{m}''_{bw} = \left(\Gamma_{\phi_c} \frac{\partial \phi_c}{\partial r} \right)_{bw} / (\phi_{c,bw} - \phi_{c,fg}) \quad ; \quad \left(\Gamma_{\phi_c} \frac{\partial \phi_c}{\partial r} \right)_{bw} = g\ (\phi_{cP} - \phi_{c,bw}) \tag{14}$$

where $\dot{m}''_{bw}$ is mass flux by the wall, the subscripts *bw* (*blowing wall*) e *fg* (*fuel grain*) are surface and inner solid fuel values, respectively, $\Gamma_{\phi c}$ is the effective transport coefficient of conserved variable (stagnation enthalpy or mixture fraction), g is a mass transfer conductance, ϕ_{cP} is near-wall value. In the present application, the conserved variable was evaluated from the solution of energy equation, thus

$$\dot{m}''_{bw} = g\,(\phi_{cP} - \phi_{c,bw})/(\phi_{c,bw} - \phi_{c,fg}) = gBP \qquad ; \qquad BP = (\tilde{H}_P - \tilde{H}_{bw})/(\tilde{H}_{bw} - \tilde{H}_{fg}) \tag{15}$$

where *BP* represents the mass transfer parameter (or blowing parameter).

Using Reynolds analogy and Couette flow approximation for the boundary layer behavior with mass transfer, the following expression can be found (Kays, 1966)

$$\tau_{bw} = \tau_w \ln(1 + BP)/BP \tag{16}$$

where τ_{bw} is wall shear stress with mass transfer and τ_w is wall shear stress for the no blowing conditions, calculated from Eq. (10) or Eq. (11).

Since the blowing rates were small for the solid fuel ramjet, the boundary conditions for κ, ε and g_f used at the adiabatic and impermeable walls also can be employed in blowing wall situations. The boundary condition for scalar conservative variable was evaluated from

$$\left(\Gamma_{\tilde{H}}\frac{\partial \tilde{H}}{\partial r}\right)_{bw} = \frac{\tau_{bw}}{\tilde{u}_P}(\tilde{H}_P - \tilde{H}_{bw}) \qquad \text{and} \qquad \left(\Gamma_{\tilde{f}}\frac{\partial \tilde{f}}{\partial r}\right)_{bw} = \frac{\tau_{bw}}{\tilde{u}_P}(\tilde{f}_P - \tilde{f}_{bw}) \tag{17}$$

The mean local regression rate can be evaluated from

$$\dot{r} = \frac{\dot{q}_w}{\overline{\rho}_{fu-s} H_{v,eff}} = \frac{H_{v,eff}\overline{\rho}_{fu-g} v_w}{\overline{\rho}_{fu-s} H_{v,eff}} \Rightarrow \dot{r} = \frac{\overline{\rho}_{fu-g}}{\overline{\rho}_{fu-s}} v_w \tag{18}$$

where $\overline{\rho}_{fu-s}$ is the solid fuel density.

4. SOLUTION PROCEDURES

The governing equations are integrated in each control volume using a finite-volume method (Patankar, 1980). The equations are discretized using the power-law scheme. The discretized set of equations was solved by means of the iterative procedure (TDMA algorithm line by line) (Patankar, 1980) using the block correction algorithm (Settari & Aziz, 1973) and under relaxation to promote convergence. The iterations are important since the equations are coupled and nonlinear. A staggered grid system is used in which the velocity components are stored at the boundaries of the control volume for the other variables. Pressure-velocity coupling was accomplished by means of the SIMPLE algorithm.

5. RESULTS AND DISCUSSION

The methodology and numerical code employed was validated by Cordeiro and Nieckele (2003) by analyzing the flow of heated air through a pipe with a sudden expansion at the inlet. The flow field inside a simplified solid fuel combustion chamber of a ramjet was also examined. The results were in good agreement with available experimental and numerical data presented in the early papers, allowing the conclusion that the model presented is suitable for the prediction of mass transfer and flow field in a solid fuel ramjet combustor.

The first case analyzed here, corresponds to the solid fuel ramjet combustor, investigated numerically by Stevenson and Netzer, (1981) and Netzer (1977) and experimentally by Boaz and Netzer (1973). The solid fuel used was PMMA (Plexiglas).

The geometric and operational parameters for the problem were the same used by Stevenson and Netzer (1981) in their simulation (L=46.28 cm, H=2.7 cm, X_{comb}=30.48 cm, R_{in}=6.81 mm and H_S=12.24 cm). The air was admitted into chamber with a temperature of 800 K, mean inlet velocity of 197.4 m/s and mass rate of 0.08049 kg/s. The solid fuel used was PMMA (Plexiglas) at a constant temperature of 700 K.

Calculations were performed using a non-uniform computational grid with 62 × 57 nodes shown in the Fig. (3). The yellow region indicates the solid fuel; therefore it is a blocked region. The radial dimension was increased to improve the visualization of results.

Figures (4) and (5) show the predicted temperature and streamlines contours in the combustion chamber region by the two models, i.e., Stevenson and Netzer (1981) and present results.

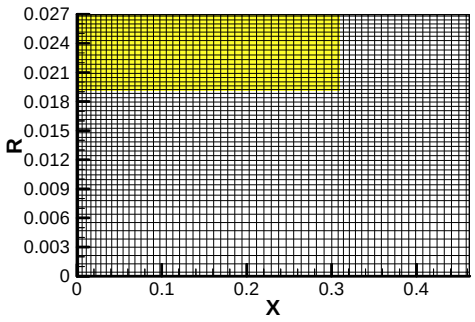

Figure 3 - Grid (in meters) used to compute flow in a solid fuel ramjet combustor.

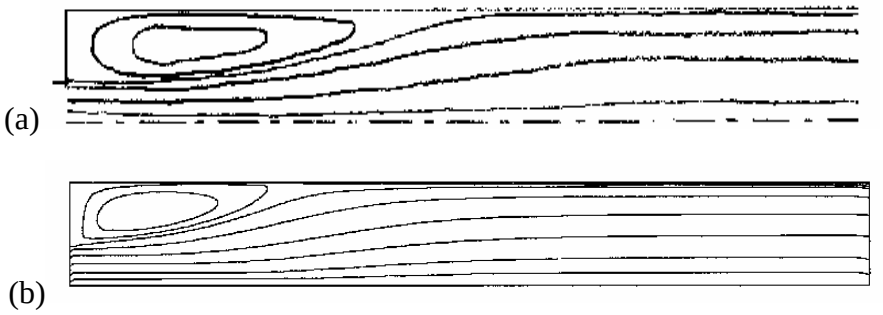

Figure 4 – Streamlines. (a) Stevenson and Netzer (1981). (b) present results.

Analyzing Fig. (4), it can be seen that the model proposed in this paper predicted a smaller recirculation zone. This behavior can be explained by the different turbulent kinetic energy boundary conditions employed in the wall functions for each model. In the Stevenson and Netzer (1981) model, the value of turbulent kinetic energy at near-wall node was calculated by its transport equation, but the source term was modified by wall shear stress value. The proposed model calculated a near-wall node turbulent kinetic energy value from the solution of transport equation at identical way for all nodes.

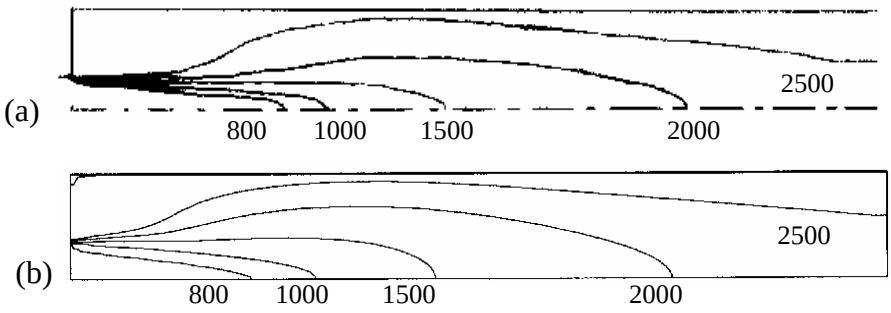

Figure 5 – Isotherms in Kelvin. (a) Stevenson and Netzer (1981). (b) present results.

It can be seen in Fig. (5), that only small differences were found between predicted temperatures contours, although the combustion models used were different. The Stevenson and Netzer (1981) model does not account for the turbulence/combustion interaction, while mixture fraction/p.d.f. formalism used in the present simulation accounts to this phenomenon. Therefore, the presented result presumes that turbulence-combustion interactions are small in this case.

Figure (6) illustrates a comparison of the temperature radial profile at two different axial coordinates. The first one is near the end of the combustor (x=30 cm) and the second is inside the after mixing region (x=38.26 cm)

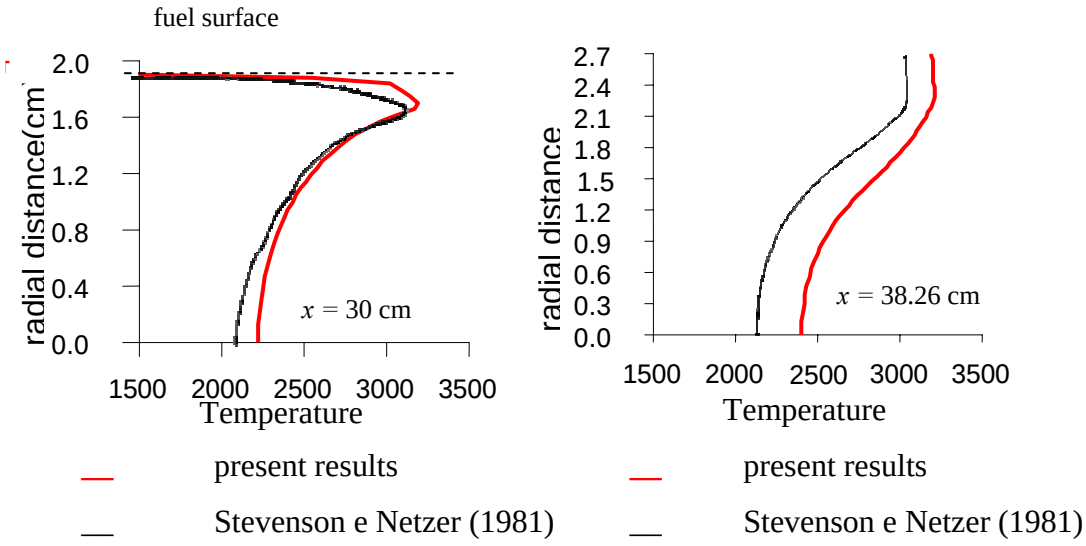

Figure 6 – Radial temperature profile.

Excellent agreement can be seen at Fig. 6a, at the axial position near the end of the fuel grain (end of the combustor). Inside the after mixing region, at a position equal to 1.5 the combustor diameter, measured from the fuel grain extremity, only similar qualitative results can be seen (Fig. 6b). Although the agreement is not as good as in the former position, the maximum deviation observed was equal to 8%. The higher temperatures predicted with the present model are due to the combustion modeled employed which takes into account the chemical-turbulence interaction. The main purposed of the after mixing region is to promote an effective mixture between the fuel and oxidant, through the creation of vortices in the recirculation region after the step, thus it was expected that the present model would represent better this phenomena. This effect is less important at the recirculation region inside the combustor, since the fuel-oxidant mixture depends of other factors, like the heat transfer from the fuel surface and the solid fuel pyrolisis.

Figure (7) shows predicted and experimental evolution of the local mean regression rate along the fuel wall. The results predicted by both models and the Netzer (1977) model were in qualitative agreement with experimental data. The behavior of predictions was similar to simplified combustor investigated by Cordeiro and Nieckele (2003). The predicted regression rate increases significantly along the centerline up to the reattachment point, and decreases farther downstream approaching a constant value. All numerical models over predicted the regression rate in the region of the flow upstream of the reattachment point and tend to underestimate the experiments that show only a very smooth peak. The over prediction of the local mean regression rate in the recirculation region can be attributed to the inability of the κ–ε turbulence model, together with the wall functions, to predict accurately the heat transfer behind a step. Since the regression rate is linearly related to the flux to the wall, the regression rate is affected by errors associated with the heat flux calculation. The models yielded qualitatively similar evolutions of the local mean regression rate along the wall, thus all evolutions exhibit the shortcomings described above if compared to the experimental data, although the predicted results were in qualitative agreement with them.

Figure (8) shows the predicted flow field for the axial velocity component and temperature within the combustor of solid fuel ramjet by the present model. Two zones of recirculation can be observed in the axial velocity flow field. The first just after the inlet step and the second one just behind the step formed at inlet of the aft mixer chamber. Since that the mixture of gaseous fuel and oxidant is more effective in the recirculation zones and combustion process is mixing limited, the higher temperatures also occur in these regions.

The fuel employed for the second case investigated was hidroxyl-terminated-polibutadiene (HTPB), commercially known as R-45. The geometric and operational parameters for the problem were based on the design of assisted ammunition (L=1.08 m, H=7.25 cm, X_{comb}=0.83 m, R_{in}=3 cm

and H_S=1.5 cm). The air was admitted into chamber with a temperature of 652.9 K, mean inlet velocity of 134.6 m/s. These data were obtained considering a flight velocity of 2.2 Mach at an altitude of 10km. The fuel employed was polimetilmecrilato (PMMA), at a constant temperature of 700 , and the pressure inside the combustor was 0,8 MPa. Calculations were performed using a non-uniform computational grid with 70 × 60 nodes with a similar distribution as in the previous case.

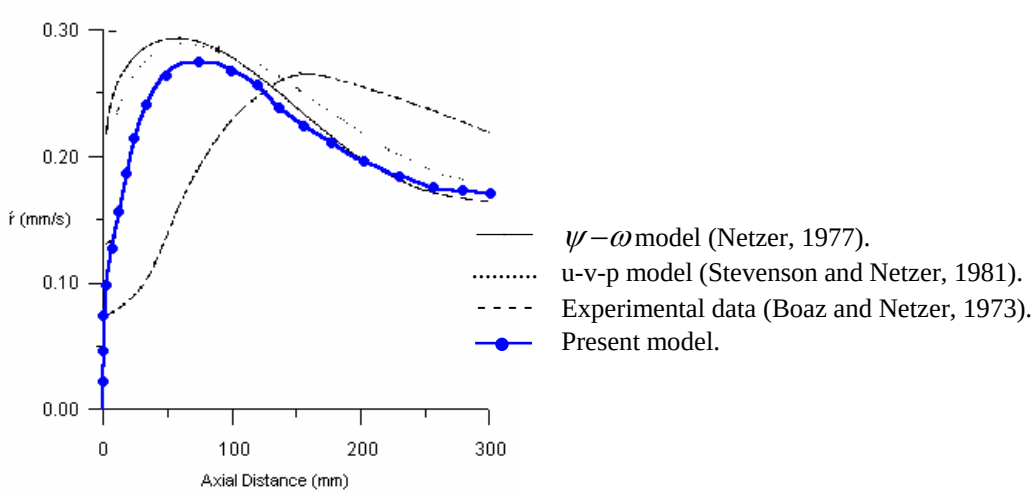

Figure 7. Regression rate along the fuel surface.

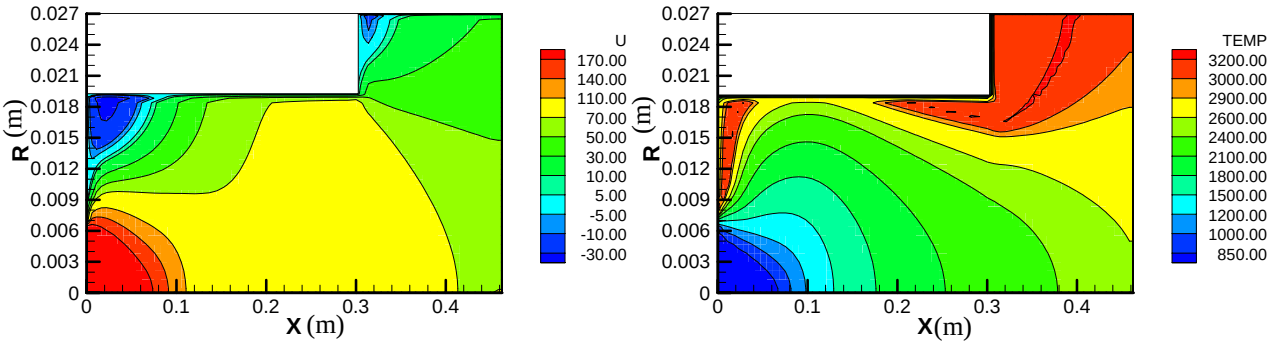

(a) Axial velocity flow field U (m/s) (b) Temperature flow field T (K)

Figure 8. Predicted flow field for axial velocity and temperature by proposed model.

The predicted flow field for the axial velocity component and temperature for the second case are shown in Fig. (9). once again, the radial dimension was increased to improve the visualization of results. It can be observed by the geometric parameters that for this case, the fuel grain length is much longer than the previous case, allowing a better development of the flow after the reattachment point. Further, the height of the entrance step is small in relation to the diameter of the air inlet orifice, and the step at the after mixture region is larger. These geometric aspects lead to a flow field with a small recirculation region near the entrance of the combustor, when compared with its dimension. On the other hand, the recirculation region behind the step at the after mixing region is larger.

Since radiation was neglected, heat transfer is due only to convection, therefore, as it can be seen in Fig. (9b), the reaction zones (regions with temperature above 2000K) are limited to the recirculation regions and the region in the neighborhood of the solid fuel. The results are similar to the previous case, with PMMA (Plexiglas). However, in that case, the recirculation region at the after mixing region was significant, indicating the presence of unburned fuel gas leaving the combustor. Therefore, the purpose of the after mixing chamber was fulfilled, enhancing the combustion efficiency, with the mixture of the oxidant and fuel, burning all fuel. At the present

case, the reaction zone at the after mixing region is small, leading to very small increase in the combustion efficiency.

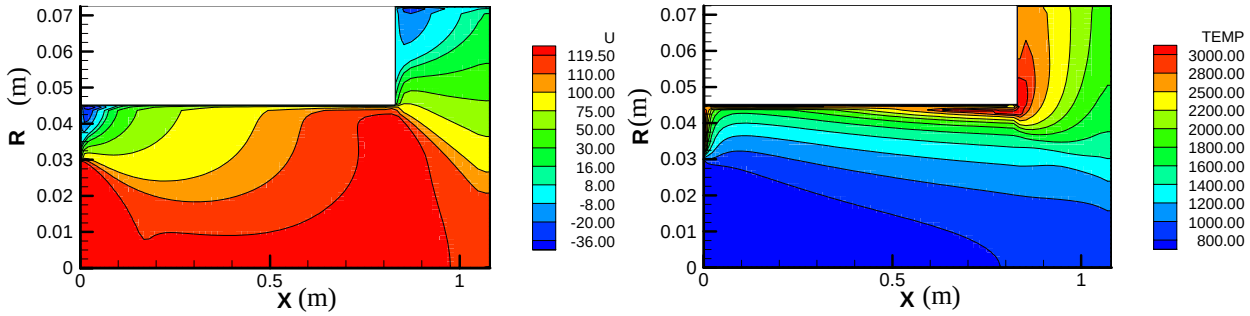

(a) Axial velocity flow field U (m/s) (b) Temperature flow field T (K)

Figure 9. Predicted flow field for axial velocity and temperature by proposed model.

Figure (10) presents the local mean regression rate of HTPB along the fuel wall. As in the previous case, there is an increase in the regression rate inside the recirculation region near the entrance of the combustor up to the reattachment point. After that the regression rate is reduced reaching an approximately constant value. The mean regression rate $\bar{\dot{r}}$ obtained was 0.33 mm/s, which is in agreement with typical experimental values of 0.25-0.35 mm/s for this type of fuel (Krishnan S.; George P., 1998). The shape of the regression rate obtained was also observed by Stevenson e Netzer (1981) e Coelho et al. (1998). As the boundary layer develops, after the reattachment point, the flame is displaced to a position far from the fuel surface, leading to the reduction of the local regression velocity. Also, the high central combustor velocity in relation to the fuel injection velocity leads to an inefficient diffusion process, reducing the air/fuel mixture in the flame zone. A similar behavior was also observed by Veras (1991), who worked with longer grains, with a larger redeveloping region.

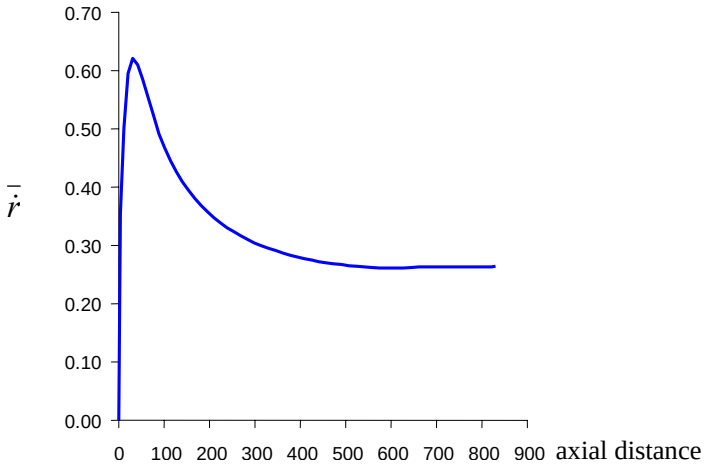

Figure 10. Regression rate along the fuel surface.

6. CONCLUSIONS

The results show that the model proposed for simulation of turbulent reactive flows in a solid fuel ramjet combustor is suitable. The evolution of the local regression rate was in qualitative agreement with experimental data. The observed discrepancies are mainly due to shortcomings of the turbulence model employed.

7. ACKNOWLEDGMENTS

Financial support for the present research was provided by CNPq.

8. REFERENCES

Boaz, L. D., Netzer, D. W., 1973, "An Investigation of the Internal Ballistics of Solid Fuel Ramjets", Naval Postgraduate School, Rept. NPS-57NT73031a.

Chatuverdi, M. C., 1963, "Flow Characteristics of Axissymmetric Expansions", J. of the Hydraulics Division, Proc. ASCE, 89, pp. 61-92.

Chieng, C. C., Launder, B. E., 1980, "On the Calculation of Turbulent Heat Transfer Downstream from an Abrupt Pipe Expansion", Numerical Heat Transfer, 3, pp. 189-207.

Ciezki H.K.; Sender J.; Clauß W.; Feinauer A.; Thumann A., 2003, "Combustion of Solid-Fuel Slabs Containing Boron Particles in Step Combustor", Journal of Propulsion and Power, AIAA, 1 November 2003, vol. 19, no. 6, pp. 1180-1191

Coelho, P. J., Duic, N., Lemos, C., Carvalho, M. G., 1998, "Modeling of a Solid Fuel Combustion Chamber of a Ramjet Using a Multi-block Domain Decomposition Technique", Aerospace Science and Technology, 2, pp. 107-119.

Cordeiro, H. M. and Nieckele, A.O. (2003) "Flow Field Computational Analysis In A Solid Fuel Ramjet Combustor", Proceedings of the 17th Brazilian Congress of Mechanical Engineering, São Paulo, Brazil, CD-ROM.

Elands, P., Korting, P., Wijckers, T., Dijkstra, F., 1990, "Comparison of Combustion Experiments and Theory in Polyethylene Solid Fuel Ramjets", J. Propulsion and Power, 6, pp. 732-739.

Gobbo-Ferreira J.; Silva M.G.; Carvalho J.A., 1999, "Performance of an experimental polyethylene solid fuel ramjet", Acta Astronautica, Elsevier Science, July 1999, vol. 45, no. 1, pp. 11-18

Kays, W. M., 1966, "Convective Heat and Mass Transfer", McGraw-Hill, pp. 300-313 and 326-328.

Krishnan S.; George P.; Sathyan S., 2000, "Design and Control of Solid-Fuel Ramjet for Pseudovacuum Trajectories", Journal of Propulsion and Power, AIAA, 1 September 2000, vol. 16, no. 5, pp. 815-822

Krishnan S.; George P., 1998, " Solid Fuel Ramjet Combustor Design", Progress in Aerospace Sciences, Elsevier Science, March 1998, vol. 34, no. 3, pp. 219-256

Launder, B. W., Spalding, D. B., 1973, "The Numerical Computation of Turbulent Flows", Computer Methods in Applied Mechanics and Engineering, pp. 269-289.

Metochianakis, M. E., Netzer, D. W., 1983, "Modeling Solid Fuel Ramjet Combustion Including Radiation to the Fuel Surface", Journal of Spacecraft and Rockets, Vol. 20, pp. 405-406.

Netzer, D. W., 1977, "Modeling Solid-Fuel Ramjet Combustion", Journal of Spacecraft, 14(12), pp. 762-766.

Patankar, S. V., 1980, "Numerical Heat Transfer and Fluid Flow", Hemisphere Publishing Corporation, Taylor and Francis Group, New York.

Pelosi-Pinhas D.; Gany A., 2003, "Bypass-Regulated Solid Fuel Ramjet Combustor in Variable Flight Conditions," Journal of Propulsion and Power, AIAA, 1 January 2003, vol. 19, no. 1, pp. 73-80

Settari, A. , Aziz, K., 1973, "A Generalization of the Additive Correction Methods for the Iterative Solution of Matrix Eq.", SIAM Journal of Numerical Analysis, Vol. 10, pp. 506-521.

Stevenson, C. A., Netzer, D. W., 1981, "Primitive-variable Model Applications to Solid-Fuel Ramjet Combustion", Journal of Spacecraft and Rockets, 18(1), pp. 89-94.

Veras, C. A. G., 1991, "Análise Experimental da Câmara de Combustão de um Estato-Reator a Combustível Sólido", Dissertação de Mestrado, Instituto Militar de Engenharia.

Wolfram, S. 2002, "The Mathematic Book", Cambrige University Press.

9. COPYRIGHT NOTICE